PLASTIC ANALYSIS OF STEEL FRAME STRUCTURE

M. Rogac
Civil Engineering Faculty, Podgorica, Montenegro
Email: mili_5@t-com.me

M. Knezevic
Civil Engineering Faculty, Podgorica, Montenegro
Email: milosknezevic@hotmail.com

M. Cvetkovska
Civil Engineering Faculty, Skopje, Macedonia
Email: cvetkovska@gf.ukim.edu.mk

ABSTRACT

This paper presents the plastic analysis of steel frame structure loaded by gravity loads. By applying the cinematic theorem of ultimate analysis, the ultimate load for the case of elastic - ideally plastic material is calculated. The identical structure was treated in the computer program SAP2000 where the zone of material reinforcement in the plastic area was covered.

Keywords: Steel frame structure, plastic analysis, ultimate gravity load, material reinforcement.

1 INTRODUCTION

For the frame structure according to Figure 1, of the welded steel cross section of columns and beams according to Figure 2, loaded by uniformly distributed gravity load on all beams, the ultimate load based on the Theory of elasticity and Theory of plasticity is calculated. [1]

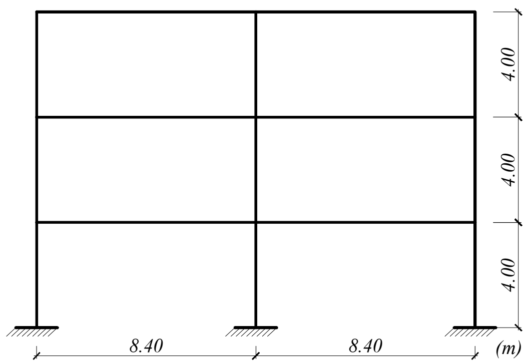

Figure 1. Frame structure layout.

Analysis of the structures according to the Theory of elasticity means the determination of the stress-deformation characteristics in the field of elastic behavior of material - zone I (Figure 3). According to [1], the ultimate load according to the Theory of elasticity, namely the load on the start of yield is q_u^e = 42.24 *kN/m*, while the maximum deflection is δ_{max}^e = 19.03 *mm*.

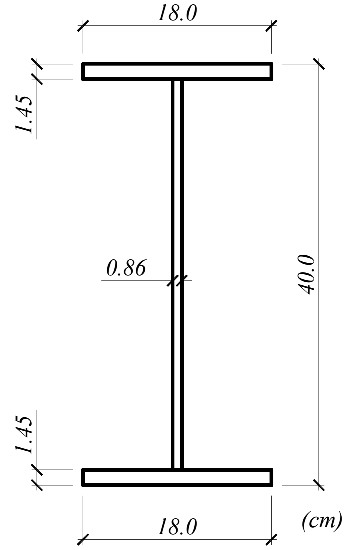

Figure 2. Columns and beams cross section.

Plastic analysis of structures enters the field of plastic behavior of material consisting of a yield zone - zone II and zone of material reinforcement - zone III (Figure 3).

The Theory of plasticity often uses approximate σ-ε diagrams that greatly simplify the problem, and are sufficiently accurate for solving of engineering problems. Figures 4 and 5 show the idealized forms of σ-ε curves used in the calculation.

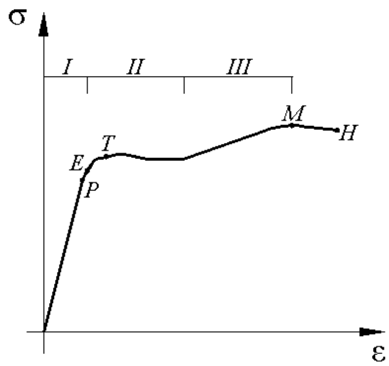

Figure 3. The actual stress-strain diagram of low carbon steel.

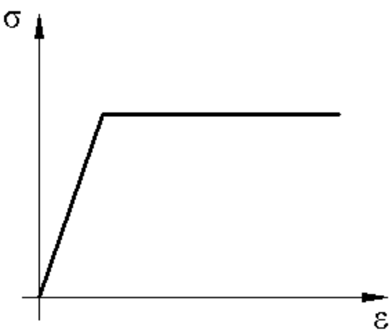

Figure 4. Elastic-ideal plastic material.

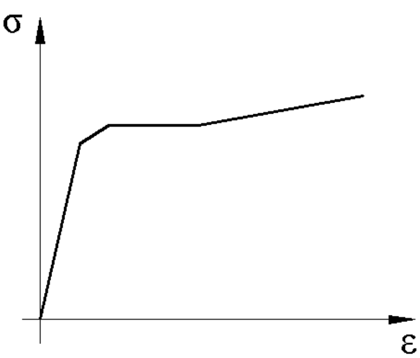

Figure 5. Elastic material with three-linear behavior in the plastic zone.

2 PLASTIC ANALYSIS

2.1 CINEMATIC THEOREM OF ULTIMATE ANALYSIS - CASE OF ELASTIC-IDEALLY PLASTIC MATERIAL

Ultimate load (q_u^p) resulting the structure collapse - formation of a local mechanism (Figure 6), is calculated using the principle of virtual displacements.

The work of external load on a virtual displacement:

$$A_s = \frac{1}{2} \cdot L \cdot \Delta \cdot q_u^{\,p} = \left(\frac{1}{2} \cdot 8.4 \cdot 4.2 \cdot \varphi \cdot q_u^{\,p} \right) \cdot 6 \qquad (1)$$

The work of internal moments on rotation in hinges:

$$\begin{aligned} A_u &= \left(M_u \cdot \varphi + 2M_u \cdot \varphi + M_u \cdot \varphi \right) \cdot 6 \\ &= \left(4 \cdot 312.5 \cdot \varphi \right) \cdot 6 \end{aligned} \qquad (2)$$

The principle of virtual displacements:

$$A_s = A_u \quad \rightarrow \quad q_u^{\,p} = 70.86 \ kN/m \qquad (3)$$

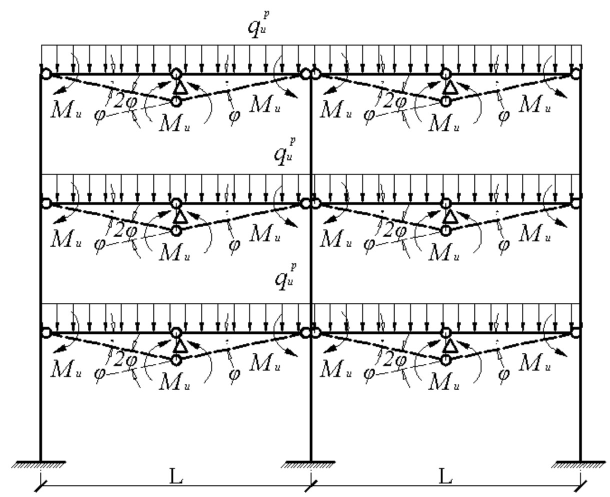

Figure 6. The collapse mechanism with indicated virtual displacement.

2.2 CALCULATION OF ULTIMATE LOAD OF THE FRAME IN THE COMPUTER PROGRAM SAP2000

In the computer program SAP2000, the behavior of the structure after the yield point is modeled with plastic hinges that can be defined in an arbitrary number of points along the length of a finite elements of the structure. Thus, the linear deformations are covered with the finite elements, and plastic deformations are covered with plastic hinges assigned to the finite elements. [2]

The formation of a plastic hinge requires a certain length at which the plastification of material will happen - the length of a plastic hinge (l_p). According to [3], for steel frame structures it is necessary to adopt a length of plastic hinge approximately equal to the height of cross section. In the analyzed example, the plastic hinges (*PZ*) of l_p = 0.4 *m* length are adopted, arranged on a mutual axial distance of 0.4 *m* on all finite elements of the structure. This ensures the possibility of plastification of all cross-sections of the structure.

Hinge property data for deformation controlled hinge are calculated based on moment-curvature diagram. For the adopted cross section (Figure 2) and σ-ε diagram from Figure 7, which represents the best approximation of actual stress-strain diagram for low carbon steel, M-φ connection is calculated using computer program XTRACT.

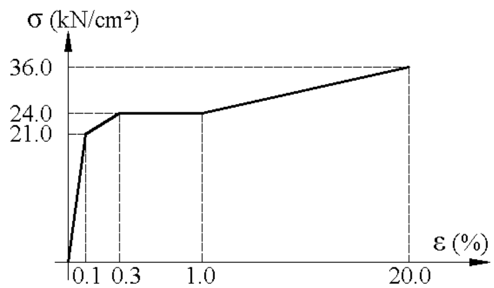

Figure 7. σ- ε diagram for low carbon steel – elastic material with three-linear behavior in the plastic zone.

Figures 8 shows XTRACT analysis report with two lines on the M-φ diagram: Actual diagram – magenta line; Effective diagram – blue line. Effective diagram is defined with two points: Yield point (Effective Yield Moment 309.0 *kNm*; Effective Yield Curvature 0.0156 *1/m*) and Ultimate point (Ultimate Moment 453.4 *kNm* = 1.4673 · EYM; Ultimate Curvature 1.025 *1/m* = 65.72 · EYC) and it is used for hinge property data calculation (Figure 9). Yield points (*B* and *B-*) are marked in magenta on the diagram and in the table, while the ultimate points (*E* and *E-*) are marked in red. Because of easier tracking of the plastic hinge status, three more points are defined on the diagram: IO – blue, LS – cyan, CP –green. Points scale factors from Figure 9 (20, 40, 60) are arbitrarily adopted.

Analysis Result:

Failing Material	5 – SD
Failure strain	.2000 Compression
Curvature at Initial Load	0 1/m
Curvature at First Yield	15.37E-3 1/m
Ultimate Curvature	1.025 1/m
Moment at First Yield	304.6 kN-m
Ultimate Moment	453.4 kN-m
Centroid Strain at Yield	11.46E-9 Compression
Centroid Strain at Ultimate	.4138E-6 Compression
N.A. at First Yield	-74.55E-6 cm
N.A. at Ultimate	-40.38E-6 cm
Energy per Length	387.1 kN
Effective Yield Curvature	15.59E-3 1/m
Effective Yield Moment	309.0 kN-m
Over Strength Factor	1.468
EI Effective	1.98E+7 N-m^2
Yield EI Effective	143.2E+3 N-m^2
Curvature Ductility	65.72

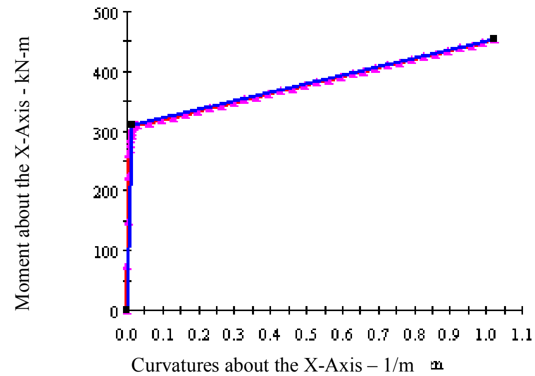

Figure 8. XTRACT Analysis Report.

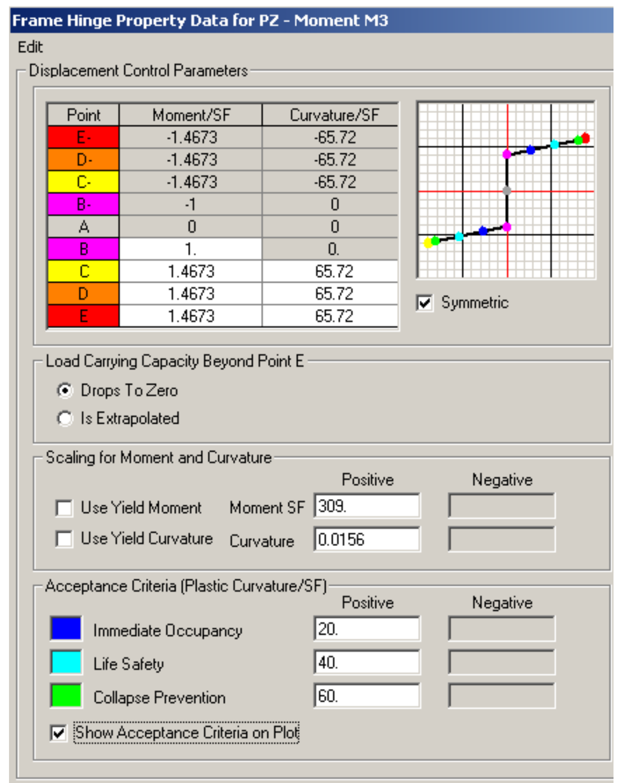

Figure 9. Frame Hinge Property Data for PZ.

By the method of testing, an ultimate uniformly distributed gravity load is determined q_u^P = 90.10 *kN/m*. During the load of 90.20 *kN/m*, a collapse mechanism has been formed and a program detects a failure in calculation.

Figure 10 shows the deformed structure with specified position and status of activated plastic hinges. Plastic hinges status is indicated by the corresponding color according to Figure 9. If the ratio of obtained curvature to Effective Yield Curvature is within 1-20 plastic hinge on Figure 10 is marked in magenta, 20-40 in blue, 40-60 in cyan and 60-65.72 in green color.

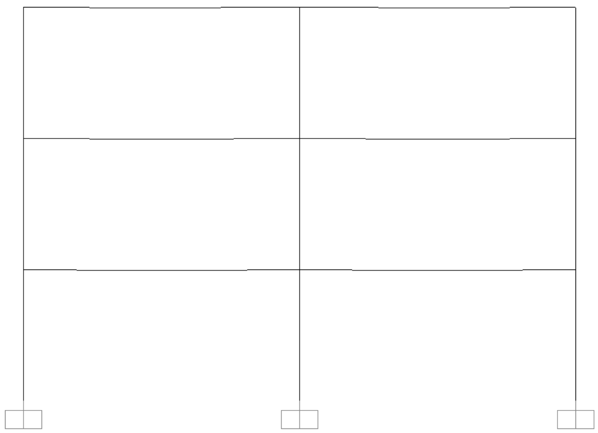

Figure 10-a. Plastic hinges are not activated - Steps 1-39.

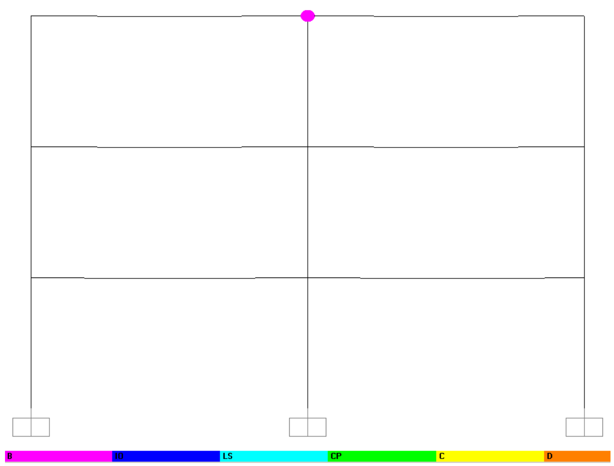

Figure 10-b. Position and status of activated plastic hinges – Step 40.

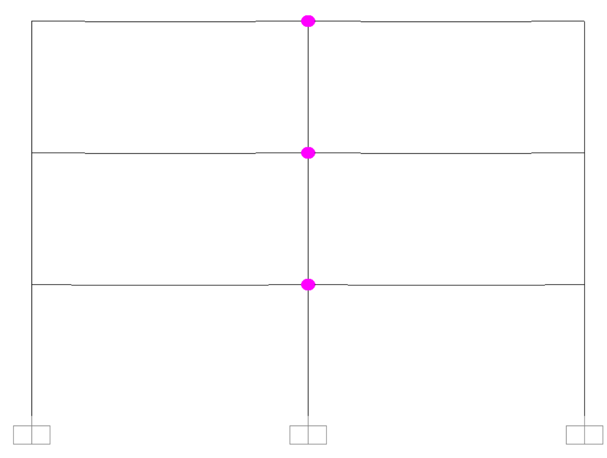

Figure 10-c. Position and status of activated plastic hinges – Step 43.

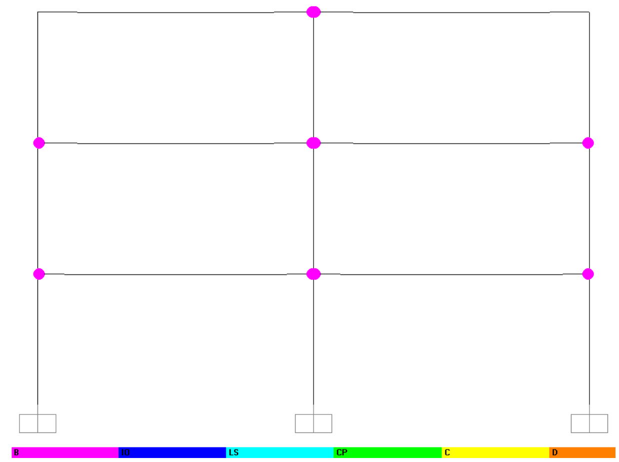

Figure 10-d. Position and status of activated plastic hinges – Step 49.

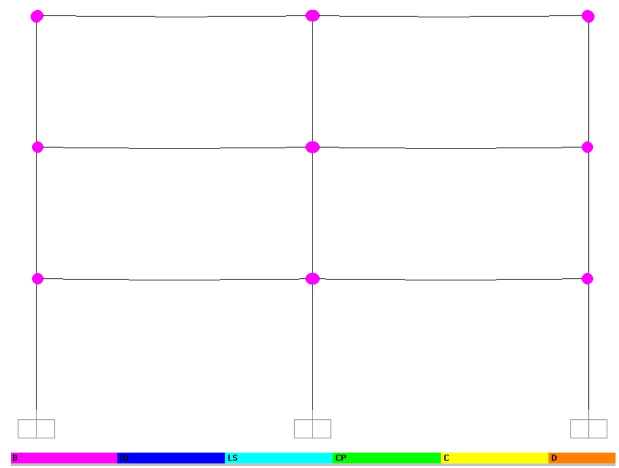

Figure 10-e. Position and status of activated plastic hinges – Step 54.

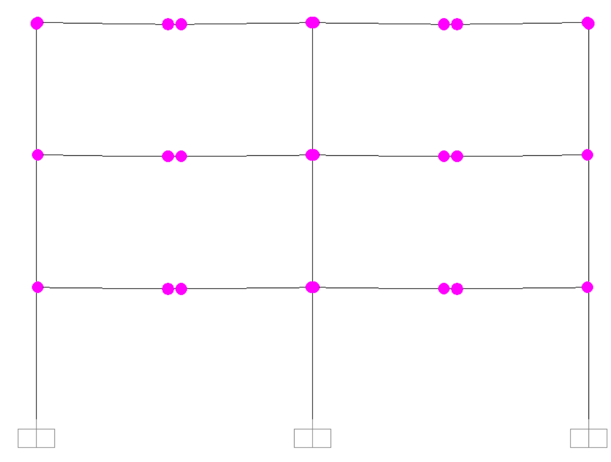

Figure 10-f. Position and status of activated plastic hinges – Step 70.

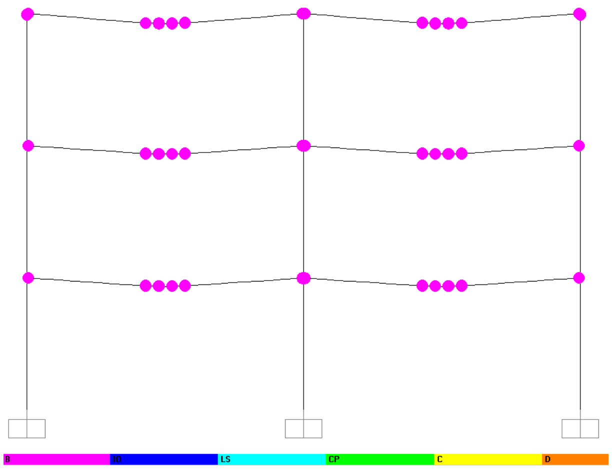

Figure 10-g. Position and status of activated plastic hinges – Step 76.

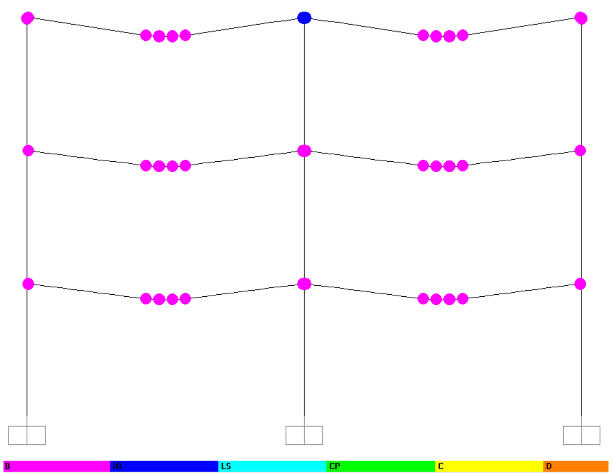

Figure 10-h. Position and status of activated plastic hinges – Step 79.

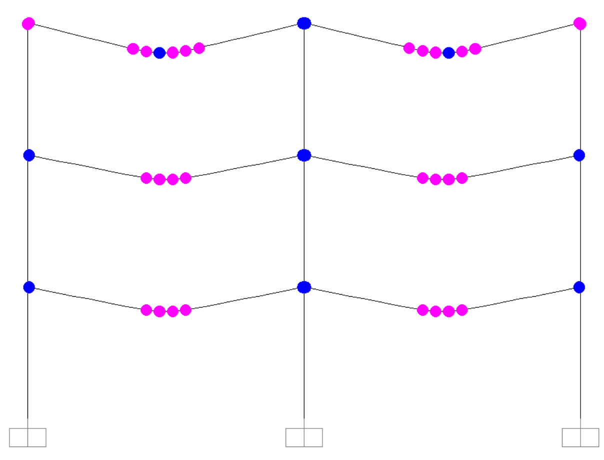

Figure 10-i. Position and status of activated plastic hinges – Step 85.

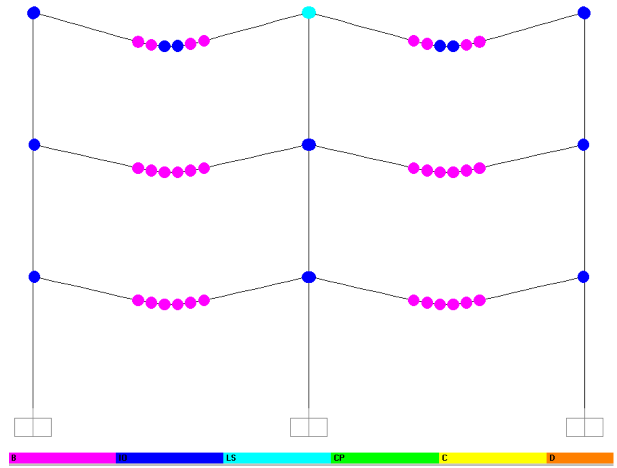

Figure 10-j. Position and status of activated plastic hinges – Step 88.

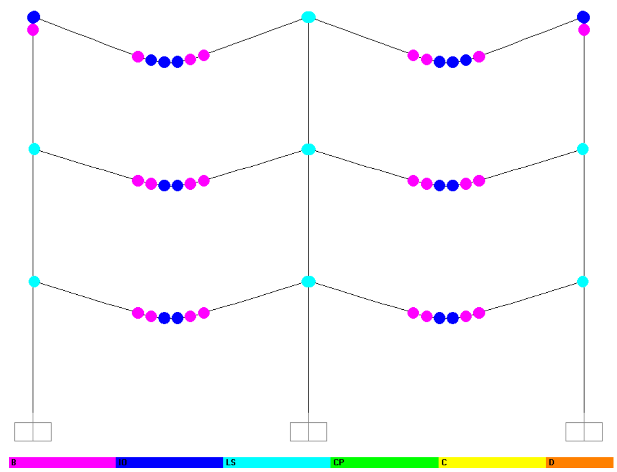

Figure 10-k. Position and status of activated plastic hinges – Step 91.

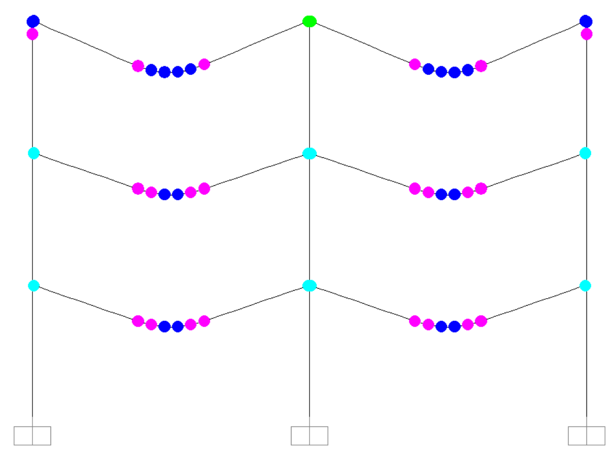

Figure 10-l. Position and status of activated plastic hinges – Step 93.

The maximum deflection under the ultimate load occurs at the center of the upper left beam according to Figure 11.

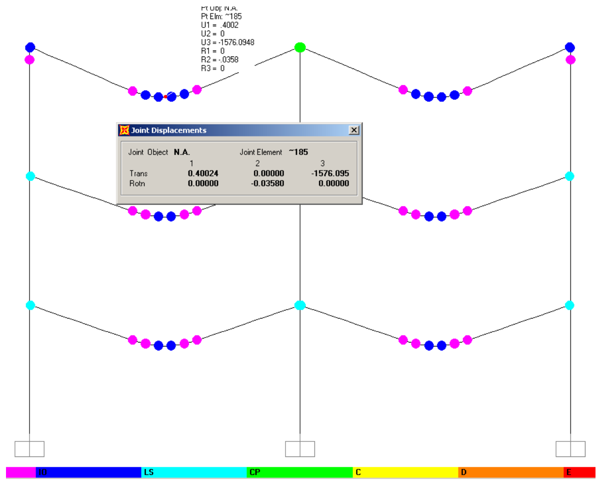

Figure 11. Maximum deflection δ_{max}^{p} = 1576 *mm*.

For all steps of analysis, it is possible to present tabular results and moment - plastic rotation diagrams (Figure 13) for all the adopted plastic hinges in the structure.

Since the curvature is defined as the rotation per length unit of the bar, the rotation of cross section *A* in relation to cross section *B* (θ_{AB}) of the bar with the change of the curvature $\varphi(x)$ is according to [4] equal to:

$$\theta_{AB} = \int_{A}^{B} \varphi(x) \cdot dx \quad (4)$$

According to [4], it is adopted that the plastic curvature ($\varphi_p = \varphi_u - \varphi_y$) has a constant value at the length of the plastic hinge (l_p) so the plastic rotation (θ_p) is equal to:

$$\theta_p = (\varphi_u - \varphi_y) \cdot l_p \quad (5)$$

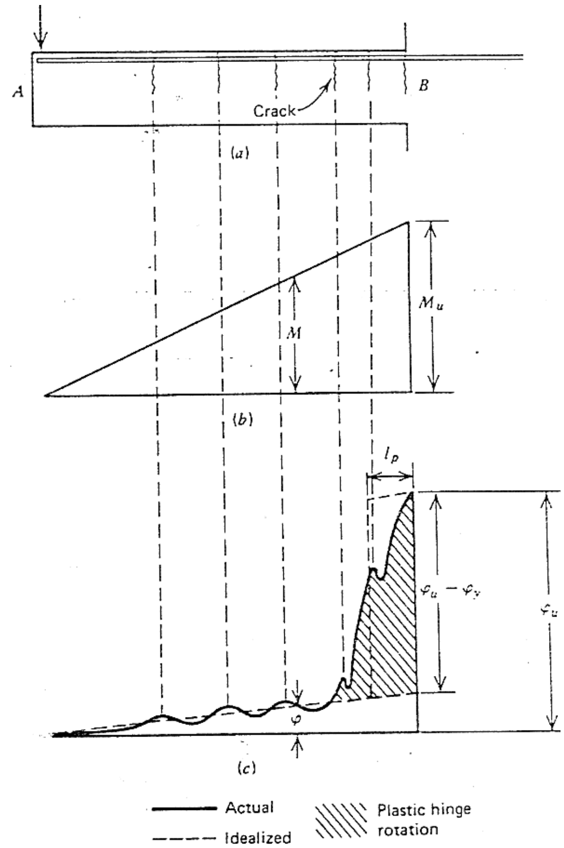

Figure 12. The displacement of curvature along the cantilever beam with ultimate moment in the fixed end: (a) cantilever, (b) bending moment diagram, (c) actual and idealized displacement of the curvature.

In the Figure 12, a concept of plastic rotation in the zone of plastic hinge is defined in the case of cantilever beam loaded by force at the free end. The hatched area represents the actual plastic rotation that occurs in the zone of formation of a plastic hinge. Dashed line is used to mark the idealized diagram - a rectangle of dimensions (φ_u-φ_y) · l_p with an area equal to hatched one. [4]

Figure 13 shows characteristic results for the plastic hinge in which plastic deformations firstly appeared (Figure 10-b). In all the steps moment and plastic rotation intensity is shown as well as plastic hinge status through the appropriate color.

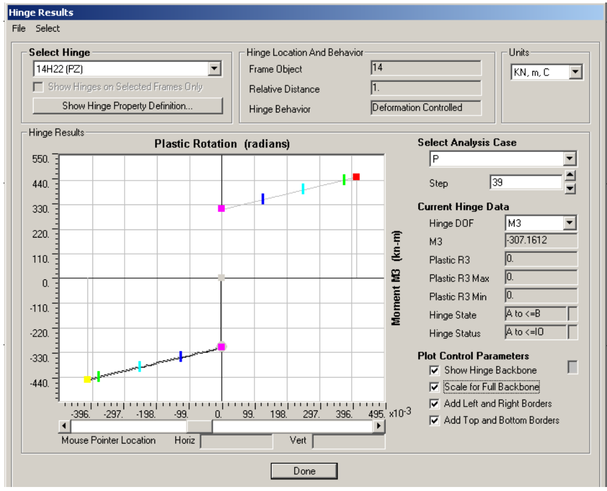

Figure 13-a. Diagram Moment-Plastic Rotation – Step 39.

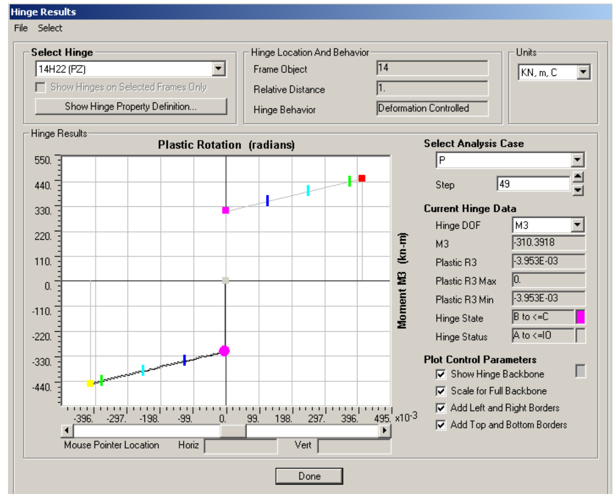

Figure 13-d. Diagram Moment-Plastic Rotation – Step 49.

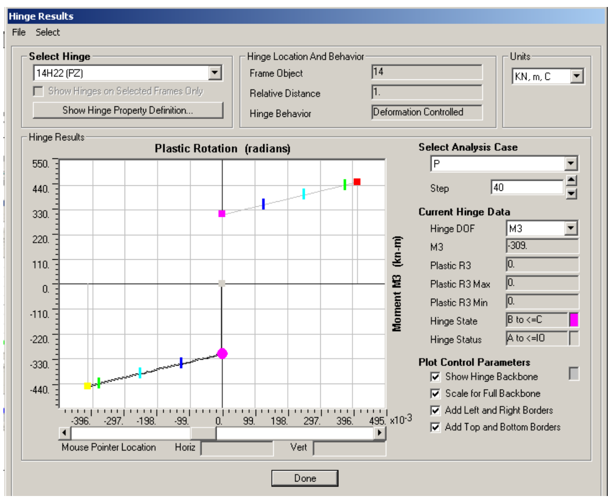

Figure 13-b. Diagram Moment-Plastic Rotation – Step 40.

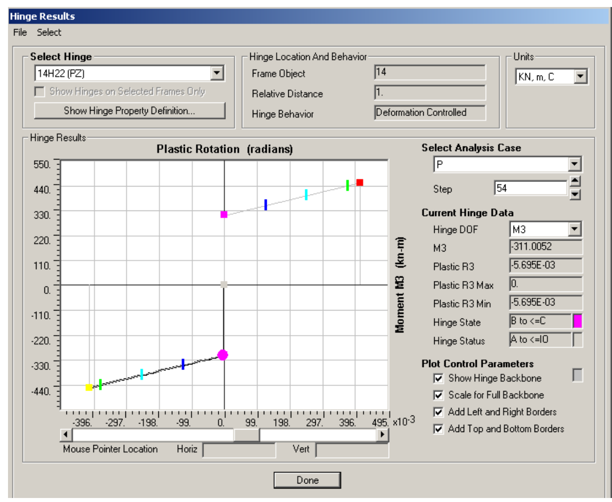

Figure 13-e. Diagram Moment-Plastic Rotation – Step 54.

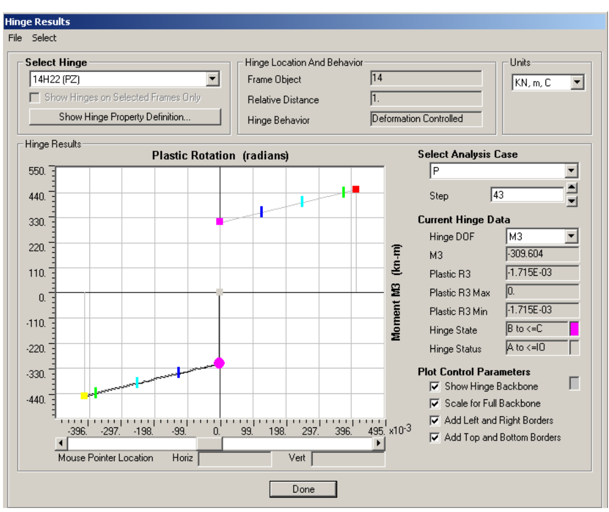

Figure 13-c. Diagram Moment-Plastic Rotation – Step 43.

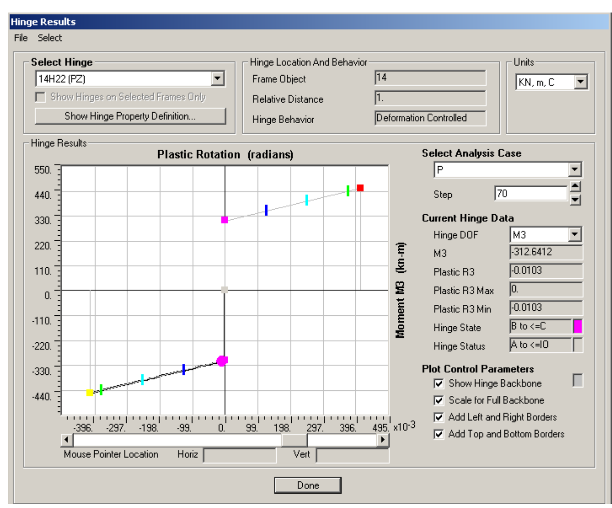

Figure 13-f. Diagram Moment-Plastic Rotation – Step 70.

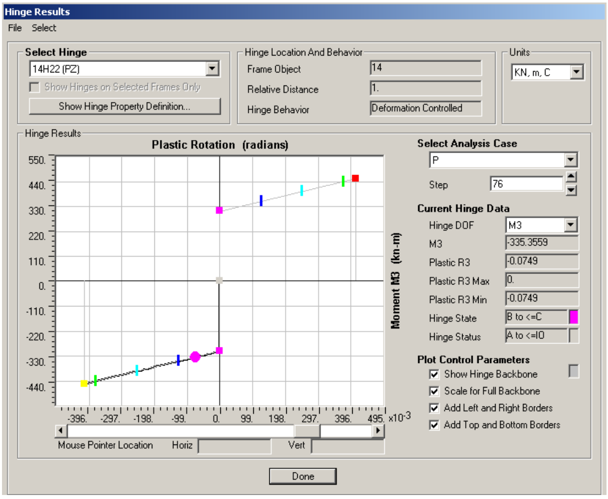

Figure 13-g. Diagram Moment-Plastic Rotation – Step 76.

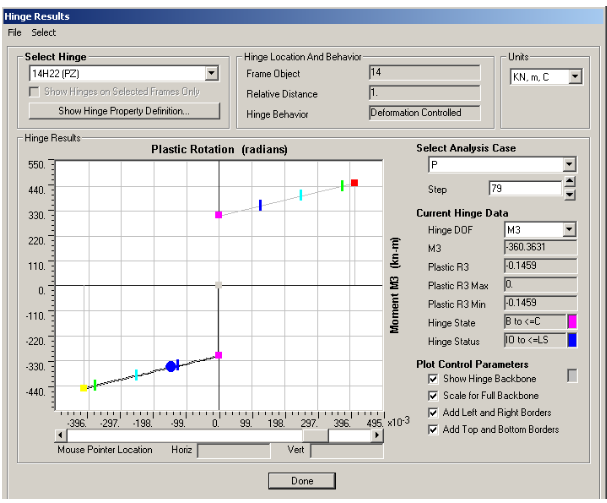

Figure 13-h. Diagram Moment-Plastic Rotation – Step 79.

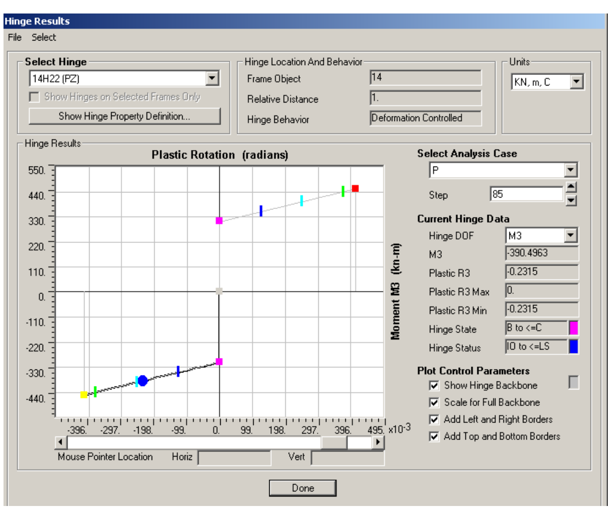

Figure 13-i. Diagram Moment-Plastic Rotation – Step 85.

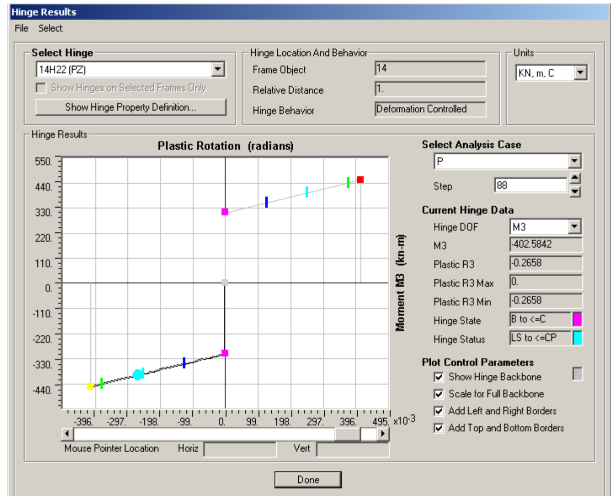

Figure 13-j. Diagram Moment-Plastic Rotation – Step 88.

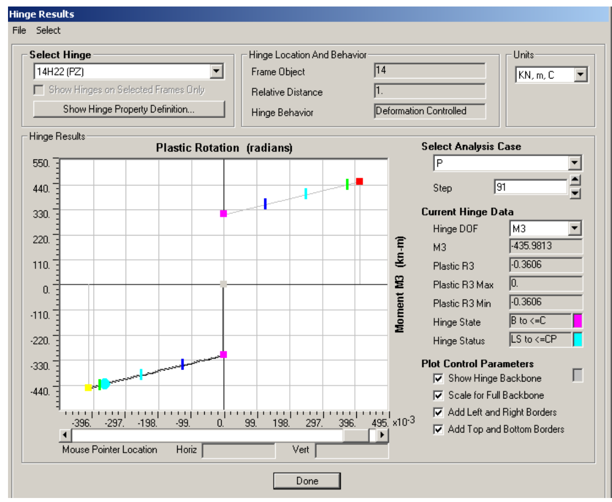

Figure 13-k. Diagram Moment-Plastic Rotation – Step 91.

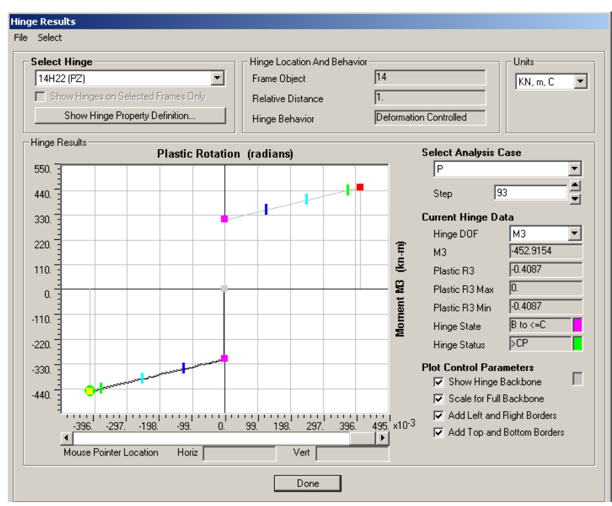

Figure 13-l. Diagram Moment-Plastic Rotation – Step 93.

3 CONCLUSION

Based on the conducted analysis, a behavior of steel frame structure loaded by the gravity load at stress levels in the plastic range can be observed.

For the case of elastic-ideal plastic material, using the cinematic theorem of ultimate analysis approximately 1.68 times bigger value of ultimate gravity load were obtained in relation to the value of ultimate load calculated according to the Theory of elasticity. Introducing the material reinforcement in the analysis, this ratio is increased to 2.13 according to Table 1. However, the deformations in the structure are multiple increased, so that in the third case, an achieved ratio of maximum span toward maximum deflection has reached a value of 5.3, and a ratio of maximum deflections according to the Theory of plasticity and Theory of elasticity is 82.82. It is therefore necessary to carefully analyze the results of plastic analysis of the structure, particularly in terms of structure usability.

The level of the obtained deformations assumes also an entry of the structure in geometric nonlinearity, not only material nonlinearity that is analyzed here. In addition, the ratio $L / \delta_{max} \approx 5.3$ involves an elastic line that has elements of a catenary with all its peculiarities in the calculation of such structures.

Plastic analysis includes large deformations, so there is a question of justification of the basic assumptions of plastic analysis, especially of Bernoulli's hypothesis of plane cross sections.

This paper analyzes the steel structure under the assumption of ideal stability of all structural elements. In further analyzes it would be interesting to introduce the influence of stability of compressed structural elements to the ultimate load.

Assumptions and idealizations mentioned in the previous two paragraphs have allowed a simple plastic analysis, and their justification should be confirmed or rejected by the experimental determination of ultimate gravity load of analyzed steel structure.

Table 1. Recapitulation of the results of conducted calculations

Method of calculation		Ultimate gravity load q_u (kN/m)	The ratio of ultimate loads according to the Theory of plasticity and Theory of elasticity	Max deflection $\delta_{\max}\ (mm)$	The ratio of the maximum span toward maximum deflection $\frac{L}{\delta_{\max}} = \frac{8400}{\delta_{\max}}$	The ratio of maximum deflection according to the Theory of plasticity and Theory of elasticity
Theory of elasticity		42.24	/	19.03	441	/
The theory of plasticity	The cinematic theorem of ultimate analysis. Elastic-ideal plastic material	70.86	1.68	/	/	/
	SAP 2000 Elastic material with three-linear behavior in the plastic zone	90.10	2.13	1576.0	5.3	82.82

REFERENCES

Rogac M.: "Plastic Analysis of Steel Frame Structure – Calculation of Ultimate Gravitational Load", *Seminar paper of the course Theory of Plasticity*, Civil Engineering Faculty in Podgorica, Podgorica, 2010, 60 p.

Computers and Structures, Inc., SAP2000® Steel Design Manual, California, USA, 2000

Sanchez L., Plumier A.: "Particularities Raised by The Evaluation of Load Reduction Factors for The Seismic Design of Composite Steel-Concrete Structures", Stability and Ductility of Steel Structures, Timisoara, 1999, 41-48 p.

Park R., Paulay T.: "Reinforced Concrete Structures", *A Wiley-Interscience Publication*, Christchurch, New Zealand, 1974, 769 p.

[this page intentionally left blank]